



IMAGE LICENSED BY INGRAM PUBLISHING

Shizhe Zang, Ming Ding,
David Smith, Paul Tyler,
Thierry Rakotoarivelo,
and Mohamed Ali Kaafar

Recently, the development of autonomous vehicles and intelligent driver assistance systems has drawn a significant amount of attention from the general public. One of the most critical issues in the development of autonomous vehicles and driver assistance systems is their poor performance under adverse weather conditions, such as rain, snow, fog, and hail. However, no current study provides a systematic and unified review of the effect that weather has on the various types of sensors used in autonomous vehicles. In this article, we first present a literature review about the impact of adverse weather conditions on state-of-the-art sensors, such as lidar, GPS, camera, and radar. Then, we characterize the effect of rainfall on millimeter-wave (mm-wave) radar, which considers both the rain attenuation and the backscatter effects. Our simulation results show that the detection range of mm-wave radar can be reduced by up to 45% under severe rainfall conditions. Moreover, the rain backscatter effect is significantly different for targets with different radar cross-section (RCS) areas.

THE IMPACT OF ADVERSE WEATHER CONDITIONS ON AUTONOMOUS VEHICLES

How Rain, Snow, Fog, and Hail Affect the Performance of a Self-Driving Car

Digital Object Identifier 10.1109/MVT.2019.2892497

Date of publication: 12 March 2019

OUR SIMULATION RESULTS SHOW THAT THE DETECTION RANGE OF MM-WAVE RADAR CAN BE REDUCED BY UP TO 45% UNDER SEVERE RAINFALL CONDITIONS.

Background

In August 2013, a Mercedes-Benz S-class vehicle called *Bertha* drove autonomously without human intervention for about 100 km from Mannheim to Pforzheim, Germany. In 2015, Tesla introduced its autopilot feature. Later, in June 2016, Google tested its fleet in autonomous mode over a total of 2,777,585 km. The fleet included the Audi TT, Toyota Prius, and Lexus RX450h, as well as Google's own cars [1]. This advanced technology not only is able to improve road safety but also relieves the burden of many tasks performed by a driver, including the following:

- self-steering with lane recognition
- distance maintenance in platooning vehicles
- self-parking
- automatic braking systems with pedestrian recognition
- notification of traffic lights, signs, and so on.

Because the on-road driving environment is very complex and dynamic, especially for navigation and control systems, most autonomous vehicles are equipped with different types of sensors. This enables driver assistance systems to exploit the respective strengths of sensors and obtain more accurate awareness of the environment by means of fusion techniques. These sensors include camera, lidar, radar, GPS, and sonar (Figure 1).

Currently, one of the most critical issues in the development of autonomous vehicles and driver assistance systems is their poor performance under adverse weather conditions, such as rain, snow, fog, and hail. In the case of adverse weather, human vision is degraded, and proper functioning of driver assistance systems becomes even more essential to drivers. Unfortunately, as in human vision, these sensors are also negatively impacted by adverse weather conditions. For example, rainy and foggy conditions cause significant degradation to the functions of camera and lidar [2]. Consequently, inaccurate information from sensors can lead to wrong decisions and, in turn, car crashes. Therefore, research on sensor performance under adverse weather conditions is particularly urgent for the development of autonomous vehicles.

Research on sensor degradation due to adverse weather conditions has emerged in recent decades. For example, [3] focused on the performance of lidar under various weather phenomena, and [4] investigated the rain effect on cameras. In [5] and [6], the authors investigated the propagation effect on mm-wave radar under various weather conditions. However, up to now, there has been no study that provides readers with a systematic and unified review about the weather effect on various types of sensors used in autonomous vehicles.

Because radar can measure the radial distance and velocity of a remote object very precisely, the market for automotive radar sensor technology is gaining momentum. According to [5], the most serious source for radar signal attenuation is rain. In [6], it is stated that backscatter also contributes significantly to the impact of rain on radar. The attenuation effect reduces the received power of useful signals, and the backscatter (clutter) effect increases interference at the receiver. Therefore, the combined effect of these two factors should be carefully investigated.

Weather Effects on Sensors for Autonomous Vehicles

Here, we review the different sensing technologies for autonomous vehicles and their respective issues under a variety of adverse weather conditions (rain, fog, snow, hail,

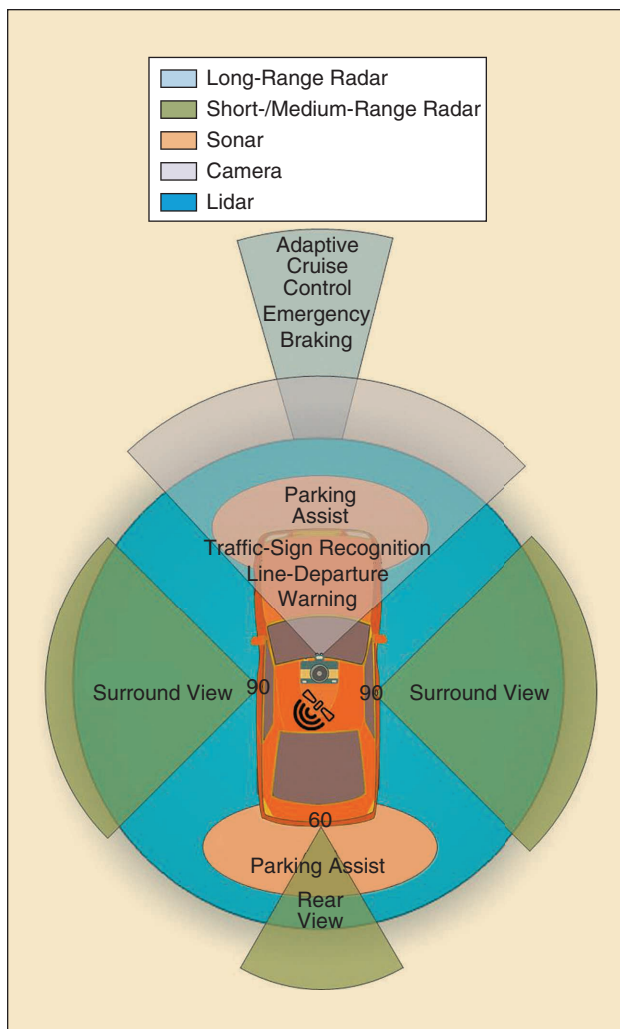


FIGURE 1 A diagram of the various sensors on an autonomous vehicle.

and space weather). The sensing technologies considered include lidar, video camera, GPS, and radar. Note that, besides the aforementioned sensors, sonar is also a popular equipment for navigation and ranging on autonomous vehicles. Because there is little performance degradation caused by weather due to short detection range [7], sonar is not considered in the following discussion.

Lidar

Because lidar sensors are able to provide outstanding angular resolution and highly accurate range measurements, in recent years, they have been proposed as an essential part of a high-performance perception system for advanced driver-assistant functions. The working principal of lidar is to first transmit a pulse and then measure the time until the lidar device receives the bounced or reflected pulse signal from a target object. The distance between the lidar device and the target is thus equal to half the round-trip time multiplied by the speed of light.

Dannheim et al. [2] proposed the criterion for object detection at the lidar receiver, i.e., that the voltage of the reflected pulse should be greater than a noise voltage threshold. From [2], the received power of lidar was affected by the extinction coefficient and the backscattering coefficient from different weather conditions. In [3], Rasshofer et al. presented the mathematical formulas to calculate these coefficients under rainy, foggy, and snowy conditions, which were determined by the distributions of particle diameters and size in relation to rainfall and snowfall rates.

The authors of [8] presented formulas about the received power and signal-to-noise ratio (SNR) of lidar with an avalanche photodiode receiver. They also investigated the relationship among peak return detection, false alarm rate, and SNR. In [8], it was mentioned that fog produced high extinction and backscattering coefficients (5×10^{-3} to 1.5×10^{-2}), which were higher than those of snowfall (10^{-3} to 5×10^{-3}) and rainfall ($< 10^{-3}$). As a result, fog had the largest impact on the detection ability of lidar.

Under rainy conditions, if the raindrop is very close to the laser emitter, there will be a high chance for false detection. This is due to the fact that, if the laser beam intersects a particle and generates a burst of light like a small surface, there will be a return of peak, which is similar to the one from an object on the road.

Some commercial products already have automatic image correction. Therefore, raindrops and snowflakes can be filtered out by pixel-oriented evaluation [9]. This involves saving sequential measurement values from each individual spot in each scan, with a separate counter being started for each spot. Erroneous measurements can be filtered out by repeatedly examining the reported area. However, there is no study on how

THE ATTENUATION EFFECT REDUCES THE RECEIVED POWER OF USEFUL SIGNALS, AND THE BACKSCATTER (CLUTTER) EFFECT INCREASES INTERFERENCE AT THE RECEIVER.

much accuracy these techniques could guarantee in adverse weather conditions.

Camera

Vehicle on-board cameras provide drivers with crucial visual signals and information for safe driving. The information can help detect pavement markings, road signs, and hazards, such as obstacles. These camera systems provide good service in more typical weather conditions, especially in clear daylight. However, system performance should not degrade in severe weather, and the camera system should continue to provide helpful information under these conditions, especially because the driver is under an increased workload. Therefore, this section analyzes the performance of camera systems in the three most frequent adverse weather conditions: snow, rain, and fog.

Rainy and Snowy Conditions

Most algorithms used in outdoor vision systems assume that intensities of image pixels are proportional to scene brightness. However, dynamic weather (rain, snow, and hail) introduces sharp intensity fluctuations in images and videos, which degrade the quality of images and videos and, thus, violate this basic assumption [10]. For example, raindrops in the air can create raindrop pattern on the image, which decreases the image intensity and blurs the edges of other patterns behind it [4]. Heavy snow and hail in the air can increase the image intensity and obscure the edges of the pattern of an object in the image or video so that the object cannot be recognized. Technologies to deal with this issue can be classified into two main categories: real-time processing and posttime processing.

In terms of real-time processing, Garg and Nayar [10] showed that, by appropriately selecting camera parameters, one could reduce (and sometimes remove) the effect of rain without appreciably altering the appearance of the scene. This was done during image acquisition and did not require any posttime processing. The work analyzed visibility of rain and then presented a method that automatically set the camera parameters (exposure time, F-number, and focus setting) to remove/reduce the effect of rain based on the analysis. For posttime processing, the authors in [11] used the deep convolutional neural network to remove rain streaks from an image. When compared with the state-of-the-art process of removing the rain from a single image, this method improved rain

COMPARED WITH MICROWAVE RADAR SYSTEMS, MM-WAVE RADAR IS ABLE TO PROVIDE HIGHER RESOLUTION.

removal and performed much faster computations after network training.

Apart from their influence on the image, raindrops, hail stones, and snowflakes can affect the camera directly. In snowy conditions, cool temperature affects a camera system because of optical and mechanical disruptions. An unshielded camera can easily be damaged by ice [12]. If the on-board camera is a powered rotation camera, such as an autotracker, the ice formed by residual moisture from rain or sleet can cause the camera to be locked in place and prevent rotation. If there is moisture around a camera below the freezing point, the frost can cover the camera's lens and prevent the viewer from seeing any activities besides the crystalline patterns of the snow. These issues can be solved by a self-heating camera, which can generate heat during its operation to avoid frozen moisture inside or on its lens. During a hailstorm, the lens of the camera can be damaged. Rainy conditions affect the system with electrical and optical malfunctions. If the system is not waterproof, it can be damaged by a short circuit from raindrops. Optically, raindrops on the lens can change the focus of the camera. As a result, part of the image affected by raindrops will be out of focus and blurred. These effects can lead to the failure of image processing, such as pattern recognition.

Foggy Conditions

Under foggy conditions, moisture (such as condensation) on a lens has a similar impact on the image processing as do snowy conditions. Furthermore, fog negatively influences perception and creates potentially dangerous situations because it can reduce the contrast of the image and increase the difficulty of pattern edge recognition [2]. In the image, sharp edges are modeled by different low and high frequencies, whereas smooth edges are characterized only by low frequencies. In the case of an observed fog scene, the frequency components are concentrated at a zero frequency, whereas, in the scene without fog, one finds a broadly spread spectrum.

The authors of [13] reviewed and compared state-of-art image enhancement and restoration methods for improving the quality and visibility level of an image using several processes: image acquisition, estimation, enhancement, restoration, and compression. From [13], the current technologies to remove fog effects were of two types: correction and removal. Fog correction was based on a change of the contrast level such as color correction. For fog removal, the fog level over an image was estimated and removed.

GPS

GPS can provide a real-time location of a vehicle, which is the core functionality for any navigation system combined with a digital map. In theory, the local weather conditions do not affect the accuracy of GPS positioning because it is designed for all weather conditions. A GPS signal frequency of approximately 1,575 MHz is chosen because it is a frequency window for signal propagation that is mostly unaffected by the weather [14]. However, vehicle GPS does suffer from some performance degradation on rainy or snowy days. For example, if a GPS module is installed inside a car attached on the windscreen, the wipers running across the windshield will intermittently block reception and make it difficult for a GPS device to detect a complete navigation data string from satellites. Therefore, the GPS may not decode the received string properly and is likely to give inaccurate information. On the other hand, if the GPS is mounted outside a car, raindrops will affect the received frequency of the GPS antenna and attenuate the signal [15].

Although GPS is not affected much by the local weather, it can be influenced by space weather (environmental conditions in solar systems). Irregularities in the ionospheric layer of Earth's atmosphere can at times lead to rapid fading in received signal power levels because of destructive interference in multipath signals. This phenomenon, referred to as *ionospheric scintillation*, can lead to a receiver being unable to track one or more visible satellites for short periods of time. Other factors affecting GPS accuracy include radio interference from other research satellites and multipath fading from the nearby environment [14]. One way to improve GPS accuracy is to enhance the receiver's tracking threshold, especially by means of external velocity aiding from an inertial measurement unit. This has already been used in some luxury cars. Other techniques include redesigning the receiver antenna and signal processing procedures.

Radar

Over the last decade, radar-based driver assistance and active safety systems have found wide applications by nearly all vehicle manufacturers in the world. The basic function of radar is for range and velocity detection of moving objects. According to American and European standards, the frequency band of the radar for automobiles is approximately 77 GHz, and the radar operating in this band is called *mm-wave radar*. When compared with microwave radar systems, mm-wave radar is able to provide higher resolution. In the mm-wave spectrum, weather conditions, such as rain, snow, mist, and hail, can have a significant impact on radar performance [5].

According to [5], the most serious source for radar signal attenuation is rain. In [6], the rain backscatter effect

was found to have a significant impact on performance. This is because droplet sizes are comparable with the radar wavelength. The attenuation effect reduces the received power of signals, and the backscatter effect increases the interference at the receiver. Radar attenuation by hail has been analyzed in [16] for microwave radar and [17] for mm-wave radar. In the event of snow or mist, mm-wave radars are also affected in the form of attenuation and backscatter. From [18], the mathematical models for attenuation and backscatter in snow and mist conditions are the same as the model in the rain condition. Next, we will investigate the rain attenuation effect, the rain backscatter effect, and their combined effect in more detail.

Rain Effects on mm-Wave Radar

As previously mentioned, rain effects on mm-wave radar can be classified into two types: attenuation and backscatter. Mathematical models of the rain attenuation effect, rain backscatter effect, receiver noise, and the combined effect will be described next.

Rain Attenuation Effect

Let r denote the distance between the radar and target. The received signal power P_r with the rain attenuation effect can be expressed as

$$P_r = \frac{P_t G^2 \lambda^2 \sigma_t}{(4\pi)^3 r^4} \cdot V^4 \exp(-2\gamma r), \quad (1)$$

where λ is the radar wavelength. Other variables are explained in Table 1. The rain attenuation coefficient γ is determined by the rainfall rate, and we consider a uniform rainfall rate between the radar and target. The rain attenuation coefficient γ can be found in [19]. The multipath coefficient V can be calculated by [5, eq. (4)].

From (1), it can be seen that we need to account for the pathloss, multipath, and rain attenuation effects when calculating the received signal power based on the transmission power. Multipath is the propagation phenomenon that results in radio signals reaching the receiver by more than one path, which is caused by reflection and refraction from objects such as buildings. The multipath effect is the interference caused by the multipath, including the constructive and destructive interferences and the phase shifting of the signal. The rain attenuation effect is determined by the rainfall rate (rain attenuation coefficient) and the distance.

Rain Backscatter Effect

According to [20, eq. (4.1)], the detection process depends on the signal-to-interference-plus-noise ratio (SINR). Maintaining the SINR above a certain threshold is vital for reliable detection. From [20, eq. (4.2)], the

RAIN EFFECTS ON MM-WAVE RADAR CAN BE CLASSIFIED INTO TWO TYPES: ATTENUATION AND BACKSCATTER.

relationship between the power intensity of the target signal and that of the backscatter signal is characterized by

$$\left(\frac{S_t}{S_b}\right) = \frac{8\sigma_t}{\tau c \theta_{BW}^2 \pi r^2 \sigma_i}, \quad (2)$$

where S_t and S_b are power intensities of the target and backscatter signals, respectively; c is the speed of light; and the other parameters are explained in Table 1. The rain backscatter coefficient σ_i is highly variable as a function of the drop-size distribution, and it can be calculated according to [21] and [24].

Although a wider beamwidth and a larger number of beams could help a radar detect more objects around a vehicle, it will also consume more power and lead to greater rain backscatter interference from (2). Therefore, it is crucial to find the optimal beamwidth for the radar based on the function requirements.

Receiver Noise

From [25], the receiver noise is given by

$$N = (F_N - 1)kT_0B, \quad (3)$$

where N is the receiver thermal noise in watts and k is the Boltzmann constant. Other variables are explained in Table 1. Although a high bandwidth provides high-range resolution for a radar and gives more accurate estimations for the target distance and speed, it also causes

TABLE 1 The simulation parameter values.

Variable	Value
P_t , transmission power	10 mW
G , antenna gain	40 dB
f , radar frequency	77 GHz
τ , pulse duration	510^{-8} s
θ_{BW} , antenna beamwidth	2°
σ_t , RCS of target	Sedan: 15.85 m^2 Pedestrian: 1 m^2
F_N , receiver noise figure	11 dB
B , receiver filter bandwidth	500 MHz
T_0 , thermal temperature	293 K

MULTIPATH IS THE PROPAGATION PHENOMENON THAT RESULTS IN RADIO SIGNALS REACHING THE RECEIVER BY MORE THAN ONE PATH, WHICH IS CAUSED BY REFLECTION AND REFRACTION FROM OBJECTS SUCH AS BUILDINGS.

noise issues for the radar receiver from (3). Therefore, there is a tradeoff in radar bandwidth, and it is important to find the optimal bandwidth for the radar receiver based on the function requirements.

The Combined Effect on mm-Wave Radar

If we treat the rain backscatter effect as interference at the receiver, the SINR can be calculated as $\text{SINR} = P_r / (P_b + N)$, where P_r is the signal power at the receiver and P_b and N are the backscatter signal power and receiver thermal

noise, respectively. Without loss of generality, we assume the areas of radar receiver and transmitter are the same. Therefore, P_r/P_b becomes the same as S_t/S_b in (2), and P_b can be calculated by using (1) and (2). Obviously, the SNR at the receiver can be written as $\text{SNR} = P_r/N$.

Simulation and Results

In this section, rain attenuation and backscatter effects on the radar detection range and received signal power are evaluated with different objects for frequency-modulation continuous-wave mm-wave radar. Four general scenarios are considered and described.

- Scenario 1: The radar detection range of a sedan is calculated versus different rainfall rates (0–400 mm/h) with fixed SINRs (10, 13, and 20 dB). The multipath effect is also considered.
- Scenario 2: The target of the radar is changed to a pedestrian, and the rest of the variables are the same as scenario 1.
- Scenario 3: A comparison between the rain attenuation and backscatter effects is performed under different rainfall rates (0–400 mm/h) with fixed distances (50, 100, and 150 m) for the detection of a sedan.
- Scenario 4: The target of the radar is changed to a pedestrian, and the fixed distances are changed to 25, 50, and 75 m. The rest of the scenario is the same as scenario 3.

The parameter values used in our simulations are summarized in Table 1. In all scenarios, the radar and target of detection can be either moving or stationary. As the rain backscatter signal power P_b is highly fluctuating with an exponential distribution, the fixed mean value is calculated in the simulations by Monte Carlo methods. The rain backscatter coefficient in the simulation is calculated according to [21, eqs. (2) and (3)] assuming the Marshall–Palmer drop-size distribution. Besides, the destructive and constructive interferences of the multipath effect in scenario 1 and 2 are modeled by random variables with exponential distributions, and the average value of the detection range is also calculated in the simulations by Monte Carlo methods.

Scenario 1: Radar Detection Range of a Sedan Versus Rainfall Rate

As mentioned, for reliable target detection, there is a requirement for the receiver SINR. The required SINR for a mm-wave radar is suggested to be 13.2 dB with a detection probability of 0.9 [22]. Therefore, in our simulation, the required SINR is set to 13 dB with multipath effect and 10, 13, and 20 dB without multipath effect.

Different detection ranges can be solved by using the SINR equation with different rainfall rates. With a given rainfall rate, the rain attenuation coefficient γ and backscatter coefficient σ_i can be calculated by [5] and [21].

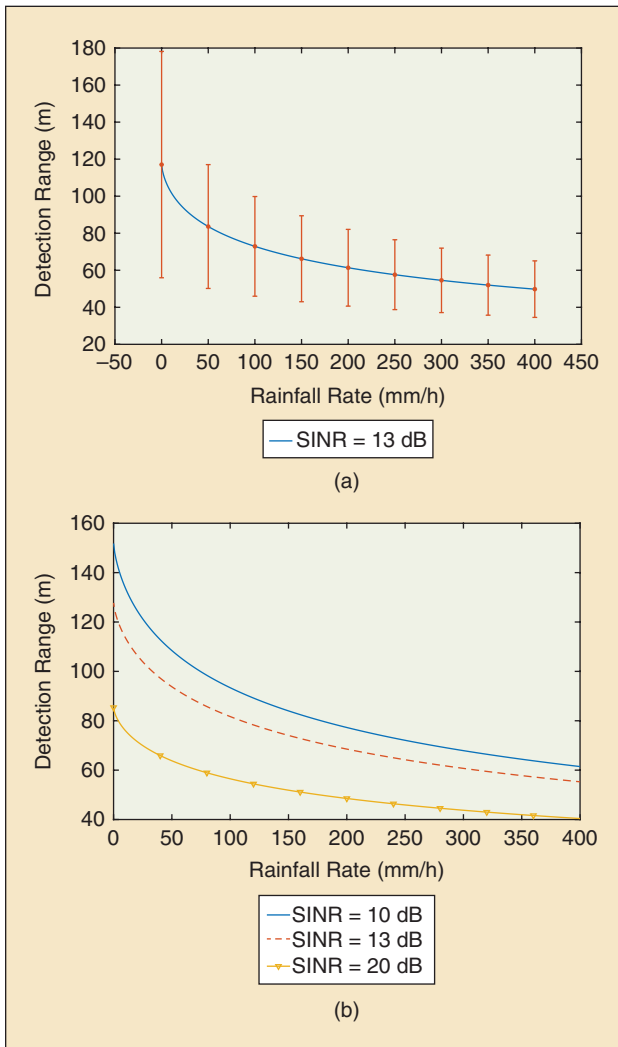


FIGURE 2 The radar detection range of a sedan versus rainfall rate (a) with the multipath effect (described by the red dashed lines) and (b) without the multipath effect.

Then, the SINR can be calculated by (1)–(3). Because the maximum rainfall rate in the world is 401 mm/h according to records, the range of the rainfall rate is set to 0–400 mm/h [23].

The simulation results are shown in Figure 2(a) with the multipath effect (described by the red dashed lines) and Figure 2(b) without the multipath effect. From Figure 2(a), it can be seen that the multipath effect (causing the variance of the detection distance) is less observable with the increase of the rainfall rate. This is because the high rainfall rate tends to attenuate the detection distance severely and leads to the reduction of the variance caused by the multipath. In Figure 2(b), it can be seen that severe and extreme rainfall conditions have a significant impact on the radar detection range. For example, when $\text{SINR} = 10$ dB, the detection range decreases 27% in severe rain conditions (50 mm/h) and 58% in extreme conditions (400 mm/h). However, when $\text{SINR} = 20$ dB, the reduction is 24% in severe conditions (50 mm/h) and 52% in extreme conditions (400 mm/h). For the normal detection requirement ($\text{SINR} = 13$ dB), the drop is approximately 25% in severe conditions (50 mm/h) and 56% in extreme conditions (400 mm/h).

Scenario 2: Radar Detection Range of a Pedestrian Versus Rainfall Rate

The difference between this scenario and the previous scenario is in the RCS area due to the change of target from a sedan to a pedestrian. The RCS is a measure of how detectable an object is by radar. In the section “Rain Attenuation Effect,” it is shown that the received power of radar is proportional to the target RCS area. Because the RCS area of a pedestrian is less than that of a sedan (see Table 1), the detection range is expected to be shorter. This is demonstrated in the simulation results presented here. We plot these simulation results in Figure 3(a) with the multipath effect and Figure 3(b) without the multipath effect. From Figure 3(a), the multipath effect of the pedestrian scenario diminishes faster than in scenario 1 because of the difference in the RCS. From Figure 3(b), the radar detection range is reduced by 26% in severe rainy conditions (50 mm/h) and 53% in extreme rainy conditions (400 mm/h) when SINR is at 13 dB. When compared with scenario 1, a target with lower RCS value experiences a faster decrease in detection range at the same SINR requirement. Furthermore, from the comparison, rainfall has a more severe impact on the detection range of a target with a smaller RCS.

From (1), it can be seen that high transmission power can provide a long detection range and high SINR . However, keeping a radar constantly on a high-power transmission mode is not energy efficient, and adaptive transmission power should be indicated based

THERE IS A TRADEOFF IN RADAR BANDWIDTH, AND IT IS IMPORTANT TO FIND THE OPTIMAL BANDWIDTH FOR THE RADAR RECEIVER BASED ON THE FUNCTION REQUIREMENTS.

on the function range and weather conditions. For instance, if rainy conditions are detected by the car (this technology is already mature for the automatic wind-screen swift), the system should increase the transmission power for the radar to reach the required SINR requirement.

Scenario 3: Radar Receiver SNR and SINR of a Sedan Versus Rainfall Rate

In this scenario, the distances between the target and the radar are fixed, and we consider attenuation and the

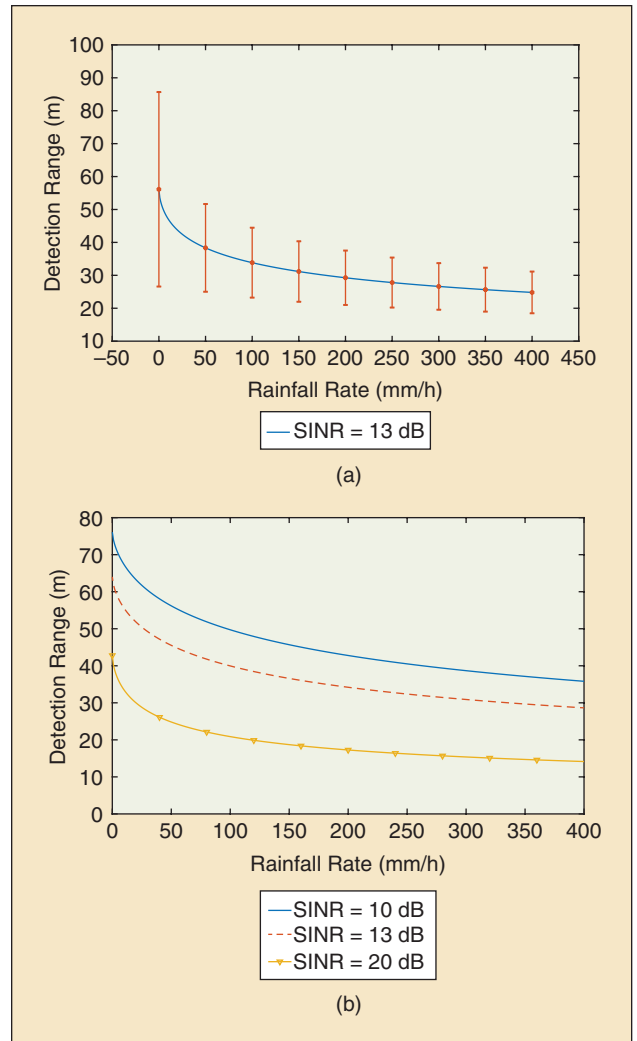


FIGURE 3 The radar detection range of a pedestrian versus rainfall rate (a) with the multipath effect (illustrated by the red dashed lines) and (b) without the multipath effect.

WITH THE INCREASE OF THE RAINFALL RATE, THE RAIN BACKSCATTER SIGNAL POWER FIRST BECOMES STRONGER AND THEN DIMINISHES DUE TO THE ATTENUATION.

backscatter effects with different rainfall rates. As mentioned previously, the SNR formulates the case where only the rain attenuation effect is considered. The SINR formulates the case where the combined effect of rain attenuation and backscatter is concerned. The receiver SNR and SINR are plotted in the same graph versus the rainfall rate. The distances are set to 50, 100, and 150 m.

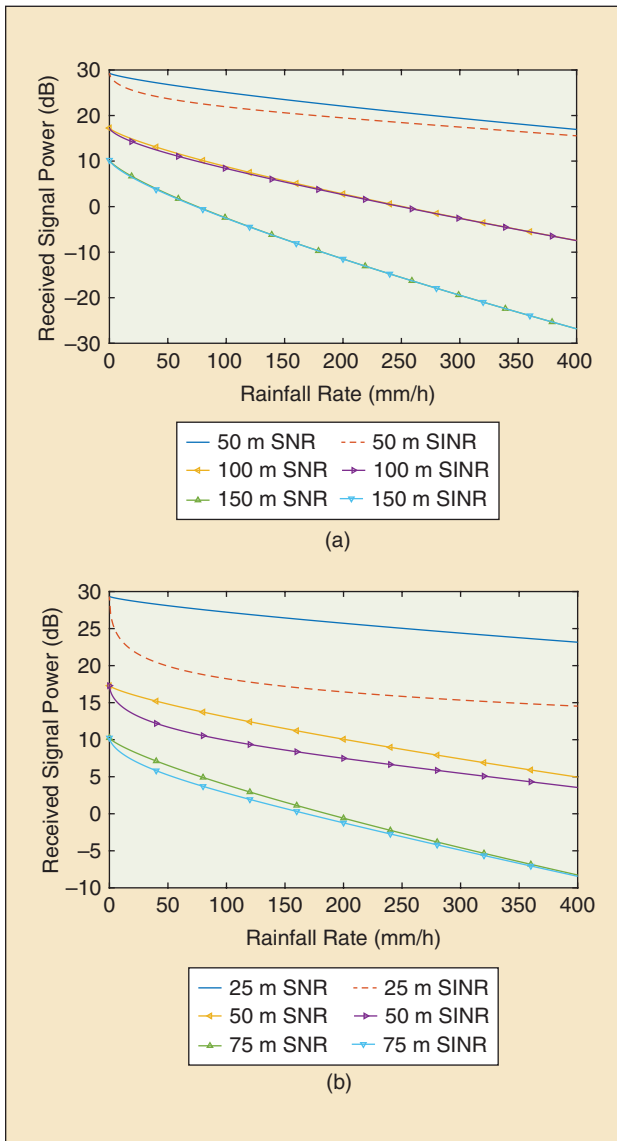


FIGURE 4 The radar receiver SNR and SINR of a (a) pedestrian and (b) sedan versus rainfall rate.

The results are shown in Figure 4(a) without the multipath effect.

From this figure, we can see that the gap between SNR and SINR first increases and then decreases with rainfall rate. With the increase of the rainfall rate, the rain backscatter signal power first becomes stronger and then diminishes due to the attenuation. Therefore, the attenuation effect is always greater than the backscatter effect on a sedan. Also, the rain backscatter effect is more obvious at a short distance from the target. This is due to the fact that backscatter from shorter distances experiences less attenuation and produces stronger interference. From a long distance, the received rain backscatter power is attenuated and is far less than the receiver noise power. This is why the curves of SINR and SNR nearly overlap at a distance of 100 and 150 m.

Scenario 4: Radar Receiver SNR and SINR of Pedestrian Versus Rainfall Rate

This scenario is similar to scenario 3 except that the target is changed from a sedan to a pedestrian. The distances between the radar and target are set to 25, 50, and 75 m as the RCS area of a pedestrian is smaller compared with a sedan. The results are shown in Figure 4(b), and the rain backscatter effect is more significant. For example, when the rainfall rate is 100 mm/h and the target distance is 25 m, the SINR degradation due to rainfall attenuation is 2.1 and 8.9 dB due to backscatter. Therefore, the backscatter effect dominates the decrease of SINR because the RCS area of a pedestrian is much smaller than a sedan. When the rainfall rate is 100 mm/h and the target distance is 50 m, the SINR degradation due to rainfall attenuation is 4 and 3 dB due to backscatter. Overall, we can conclude that backscatter has more impact on the radar performance at a short distance while attenuation has more impact on the radar performance at a long distance.

Conclusions

This article provides a literature review about the influence of adverse weather conditions on state-of-the-art sensors, such as lidar, GPS, camera, and radar. Furthermore, we characterize the effect of rainfall on automotive radar, which considers both the attenuation and backscatter effects. The simulation results show that the detection range of a mm-wave radar can be reduced by up to 45% under severe rainfall conditions (150 mm/h). Moreover, for a close-range target with a small RCS area, the backscatter effect plays a more significant role, causing additional performance degradation.

Author Information

Shizhe Zang (shizhe.zang@sydney.edu.au) is a Ph.D. degree candidate at the Centre of Excellence in Internet



of Things and Telecommunication, University of Sydney, Australia. His current research interests include the Internet of Things and mobile edge computing.



Ming Ding (ming.ding@data61.csiro.au) is a senior research scientist with Data61, the Commonwealth Scientific and Industrial Research Organisation, Australia. His research interests include information technology, data privacy and security, and wireless communications. He is a Senior Member of the IEEE.



David Smith (david.smith@data61.csiro.au) is a principle research scientist with Data61, the Commonwealth Scientific and Industrial Research Organisation, Australia, and an adjunct fellow with Australian National University. His research interests are in body area networks, game theory for distributed networks, disaster tolerant networks, 5G, the IoT, smart grid optimization, and privacy for networks. He is a Member of the IEEE.



Paul Tyler (paul.tyler@data61.csiro.au) is a senior research engineer with the Network Research Group, Data61, the Commonwealth Scientific and Industrial Research Organisation, Australia. His research interests include systems engineering, computer systems administration, and software development.



Thierry Rakotoarivelo (thierry.rakotoarivelo@data61.csiro.au) is a senior research scientist with the Network Research Group, Data61, the Commonwealth Scientific and Industrial Research Organisation, Australia. His research interests include peer-to-peer mechanisms to discover and utilize quality of service-enhanced alternate paths on the Internet and protocols and frameworks for large-scale distributed testbeds (i.e., design, provisioning, control/orchestration, and instrumentation).



Mohamed Ali Kaafar (dali.kaafar@mq.edu.au) is the group leader of the Information Security and Privacy Group, a senior principal researcher with Data61, the Commonwealth Scientific and Industrial Research Organisation, Australia, and the scientific director at Optus Macquarie Cyber Security Hub, Macquarie University, Sydney, Australia. His research inter-

ests include data privacy, network security, and performance modeling.

REFERENCES

- [1] Wikipedia, "Waymo: Google self-driving car." Accessed on: Jan. 29, 2019. [Online]. Available: <https://en.wikipedia.org/w/index.php?oldid=736369985>
- [2] C. Dannheim, C. Icking, M. Mader, and P. Sallis, "Weather detection in vehicles by means of camera and LIDAR systems," in *Proc. IEEE Computational Intelligence, Communication Systems and Networks (CICSyN)*, 2014, pp. 186–191.
- [3] R. H. Rasshofer, M. Spies, and H. Spies, "Influences of weather phenomena on automotive laser radar systems," *Adv. Radio Sci.*, vol. 9, pp. 49–60, July 2011.
- [4] A. Cord and N. Gimonet, "Detecting unfocused raindrops: In-vehicle multipurpose cameras," *IEEE Robot. Autom. Mag.*, vol. 21, no. 1, pp. 49–56, Mar. 2014.
- [5] G. P. Kulemin, "Influence of propagation effects on millimeter wave radar operation," in *Proc. SPIE Conf. Radar Sensor Technol.*, vol. 3704, Apr. 1999, pp. 170–178.
- [6] H. B. Wallace, "Millimeter-wave propagation measurements at the ballistic research laboratory," *IEEE Trans. Geosci. Remote Sens.*, vol. 26, no. 3, pp. 253–258, May 1988.
- [7] B. Yamauchi, "All-weather perception for man-portable robots using ultra-wideband radar," in *Proc. 2010 IEEE Int. Conf. Robotics and Automation (ICRA)*, May 2010, pp. 3610–3615.
- [8] L. Hespel, N. Riviere, T. Huet, B. Tanguy, and R. Ceolato, "Performance evaluation of laser scanners through the atmosphere with adverse condition," in *Proc. SPIE*, vol. 8186, 2011.
- [9] SICK, "Lasermessungssystemtechnicaldescription," 2019. [Online]. Available: <http://sicktoolbox.sourceforge.net/docs/sick-lms-technical-description.pdf>
- [10] K. Garg and S. K. Nayar, "When does a camera see rain?," in *Proc. 10th IEEE Int. Conf. Computer Vision (ICCV'05)*, vol. 2, Oct. 2005, pp. 1067–1074.
- [11] X. Fu, J. Huang, X. Ding, Y. Liao, and J. Paisley, "Clearing the skies: A deep network architecture for single-image rain removal," *IEEE Trans. Image Process.*, vol. 26, no. 6, pp. 2944–2956, June 2017.
- [12] J. Nava, "Weather affects surveillance cameras," Security Camera King, Boca Raton, FL, 2019. [Online]. Available: <http://www.security-cameraking.com/securityinfo/weatheraffectsurveillance-cameras/>
- [13] G. Yadav, S. Maheshwari, and A. Agarwal, "Fog removal techniques from images: A comparative review and future directions," in *Proc. 2014 Int. Conf. Signal Propagation and Computer Technology (ICSPCT)*, July 2014, pp. 44–52.
- [14] E. Kaplan and C. Hegarty, *Understanding GPS: Principles and Applications*, Norwood, MA: Artech House, 2005.
- [15] J. Mehafeey, "Rain, snow, clouds and GPS reception," 2019. [Online]. Available: <http://www.gpsinformation.net/gpsclouds.htm>
- [16] L. J. Battan, "Radar attenuation by wet ice spheres," *J. Appl. Meteorol.*, vol. 10, no. 2, pp. 247–252, 1971.
- [17] R. Lhermitte, "Attenuation and scattering of millimeter wavelength radiation by clouds and precipitation," *J. Atmos. Oceanic Technol.*, vol. 7, no. 3, pp. 464–479, 1990.
- [18] V. N. Pozhidaev, "Estimation of attenuation and backscattering of millimeter radio waves in meteorological formations," *J. Commun. Technol. Electron.*, vol. 55, no. 11, pp. 1223–1230, 2010.
- [19] R. Olsen, D. V. Rogers, and D. Hodge, "The aRb relation in the calculation of rain attenuation," in *IEEE Trans. Antennas Propag.*, vol. 26, no. 2, pp. 318–329, Feb. 1978.
- [20] S. Hovanessian, *Introduction to Sensor Systems*, Norwood, MA: Artech House, 1988.
- [21] J. Huang, S. Jiang, and X. Lu, "Rain backscattering properties and effects on the radar performance at mm wave band," *Int. J. Infrared Millimeter Waves*, vol. 22, no. 6, pp. 917–922, 2001.
- [22] Australian Centre for Field Robotics, University of Sydney, "Chapter 10. Detection of signal in noise," Accessed on: Aug. 28, 2016. [Online]. Available: <https://pdfs.semanticscholar.org/67e5/45a70152ebc11c9e7fdef90e88f37742474.pdf>
- [23] World Meteorological Organization, "World's record rainfall," 2019. [Online]. Available: <http://www.bom.gov.au/water/designRainfalls/rainfallEvents/worldRecRainfall.shtm>
- [24] R. J. Doviak and D. S. Zrnić, *Doppler Radar and Weather Observations*. Mineola, NY: Courier Corporation, 2006.
- [25] J. C. Toomay, *Radar Principles for the Non-Specialist*, vol. 2. Dordrecht, The Netherlands: Springer, 2004.

VT